Environ Geol (2008) 54:1271–1281
DOI 10.1007/s00254-007-0909-1

ORIGINAL PAPER

Influence of pore system characteristics on limestone vulnerability: a laboratory study

G. Cultrone · L. G. Russo · C. Calabrò · M. Uroševič · A. Pezzino

Received: 30 April 2007 / Accepted: 20 June 2007 / Published online: 12 July 2007

Abstract Hyblean limestone of Oligo-Miocene age was widely used as a construction material in the architectural heritage of Eastern Sicily (Italy). Among them, the so-called Pietra Bianca di Melilli (Melilli limestone) and Calcare di Siracusa (Syracuse limestone) were prized for their attractive appearance, ease of quarrying, and workability. Syracuse limestone shows general weathering, whereas Melilli limestone is better preserved, and only differential erosion or superficial exfoliation can be detected in monuments. The cause of the different behavior of these two limestones was investigated from the petrographic and petrophysical points of view. The saturation coefficient is higher in Melilli limestone, and ultrasound measurements indicate that it is less compact than Syracuse limestone, so that Melilli limestone could deteriorate more easily than Syracuse limestone. However, pore interconnections and the size of very small pores play the main role in the durability of both materials. The "irregularity" of the Syracuse pore system and its greater number of micropores hinder water flow through the exterior, promote stress in pore structure, and favor the development of scaling, as confirmed by salt crystallization tests. In Melilli limestone, the low concentration of micropores and fast water evaporation allow solutions to reach the surface more easily, resulting in less damaging efflorescence.

G. Cultrone (✉) · M. Uroševič
Department of Mineralogy and Petrology,
University of Granada, Avda, Fuentenueva,
18002 Granada, Spain
e-mail: cultrone@ugr.es

L. G. Russo · C. Calabrò · A. Pezzino
Department of Geology,
University of Catania,
Corso Italia 57, 95100 Catania, Italy

Keywords Limestones · Pore system · Crystallization pressure · Durability

Introduction

Hyblean limestone was the main construction material used in the Architectural Heritage of Eastern Sicily (Italy). All the lithotypes, belonging to various geological formations, are commercially known as "Pietra di Siracusa" (Syracuse stone). This is because, in the past, names were not associated with the petrologic features of the stone, but with the location of quarries. Within the family of Syracuse stone, the Oligo-Miocene limestone of the Monti Climiti Formation was extensively used to build important artistic monuments in the Syracuse and Catania districts, which today suffer from various kinds of deterioration.

The Monti Climiti Formation is divided into two geological members:

1. Syracuse limestone member, still known as *Pietra di Siracusa*.
2. Melilli member, also known as *Pietra Bianca di Melilli* (Melilli white stone).

Syracuse limestone (henceforth SL) has an older origin as a construction material, and was indeed used to build monuments of Greek and Roman age in the city of Syracuse. In chronological order, we mention the Temple of Apollo (early sixth century BC), the Temple of Athena (mid-sixth century BC), the Greek Theatre (fifth century BC) and the Castle of Eurialo (402–397 BC).

The ancient quarries from which SL comes are known as *latomie* (i.e., stone quarries). There are 12 *latomie*, all located around the city of Syracuse.

After the earthquake of 1693, which destroyed the eastern area of Sicily, Melilli limestone (henceforth ML) was quarried to build civic and religious monuments in Melilli (e.g., Mother Church, Church of the Holy Ghost and City Council building), and in Syracuse (e.g., Old Market Palace, Municipal Theatre).

The aims of this work are to characterize the limestones of these two geological members from the mineralogical and petrophysical points of view, and to identify the causes of the different decay in ancient monuments.

Geological setting

The Hyblean Plateau is a thick Triassic to Quaternary carbonate platform in the SE part of Sicily (Grasso 1997), representing an emerging portion of African continental crust (Catalano et al. 2000) forced back down under the Appennine-Maghrebian thrust belt (Grasso et al. 1982). Two main fault systems crosscut this plateau: one, extensional trends NE-SW, the other, trending NNW-SSE, mostly consists of strike-slip faults (Ragg et al. 1999). The Hyblean plateau is mainly composed of Oligo-Miocene sedimentary sequences belonging to the Ragusa Formation to the west and to the Sortino Group (Grasso et al. 1982), which comprises the formations of the Monti Climiti, Carlentini and Monte Carrubba Formations, to the east (Fig. 1).

The Ragusa Formation is divided in two members: Leonardo and Irminio (Rigo and Barbieri 1959). The Leonardo Member (Oligocene to Aquitanian in age) consists of well-bedded alternating sequences of whitish-gray to cream planktonic foraminifera biomicrite with marly planctonic foraminifera biomicrite. The Irminio Member (Aquitanian-Burdigalian) shows a regular succession between marl and biomicrite (Pedley 1981). Gradually, sedimentation evolved from the Middle Miocene marl of the Tellaro Formation, which is partially heterotopic, to the Tortonian biocalcarenite of the Palazzolo Formation (Grasso et al. 1979).

The Monti Climiti Formation (Upper Oligocene–Lower Miocene) is composed of two members: the lower, Melilli, consists of yellowish wackstone with planktonic foraminifera; the higher, Syracuse, comprises white coloured packstones with molluscs, echinoids and sporadic *porites* (Pedley 1981).

Basaltic volcanic activity occurred intermittently, with carbonate depositions, from the late Triassic to the early Pleistocene, in an environment characterized by eustatic and isostatic sea-level fluctuations and active tectonism (Carbone and Lentini 1981). Lastly, in the early Messinian, the area was affected by progressive subsidence and the deposition of the Monte Carrubba Formation, a limestone with restricted fauna (*Pectinidae* and *Cardidae*) (Grasso and Lentini 1982; Yellin-Dror et al. 1997).

Materials and methods

Study methods include two steps:

(a) macroscopic observation of the monuments in the cities of Syracuse and Melilli to identify lithotypes, to recognize decay forms, and to establish the degree of deterioration;
(b) mineralogical and petrophysical analyses on samples collected from quarries. Two historical quarries were selected near Melilli: "Palombara" for Syracuse limestone and "Pirrera di Melilli" for Melilli limestone. These are the only quarries in the area in which the two lithotypes were excavated in blocks.

The mineralogy and texture of limestone samples were analyzed under a Zeiss Axiolab polarized optical microscope. Thin sections were prepared and observed with parallel and crossed nicols.

Insoluble limestone residues were studied as follows: (1) $CaCO_3$ was removed by a dilute sodium acetate–acetic acid solution (pH 5) on finely milled samples; (2) insoluble residues were granulometrically divided into sand (2 mm<∅<62.5 μm), silt (62.5 μm<∅<4 μm) and clay (∅<2 μm) fractions using an ALC® PK 110 spin-drier; (3) the resulting mineralogical composition of the fractions was determined by powder X-ray diffraction (Siemens D-5000 XRD), with automatic slit and Cu$K\alpha$ radiation. Analysis conditions were 0.02° 2θ s^{-1} goniometer speed; 5 to 45° 2θ explored area for ∅>2 μm fraction, and 3 to 35° 2θ for ∅<2 μm fraction. The XRD of the clay fraction was performed using oriented aggregates: air-dried (untreated), solvated for 48 h at 60°C with ethylene glycol (Bruton 1955) and heated for 1 h at 550°C (Moore and Reynolds 1989).

The parameters associated with water uptake and transport inside limestone pores were determined by hydric tests. Since the degree of mechanical resistance and decay processes often depend on water circulation inside porous solids (Charola and Lazzarini 1986; Kowalski 1975), these tests were important to determine the durability of these limestones. Water absorption (NORMAL 7/81 1981), drying (NORMAL 29/88 1988) and capillary uptake (UNI-EN1925 2000) were determined by weighing the samples (three samples per lithotype) at regular intervals. The absorption coefficient, drying index, real and apparent density, saturation coefficient, degree of pore interconnectivity, and open porosity were calculated from the values thus obtained.

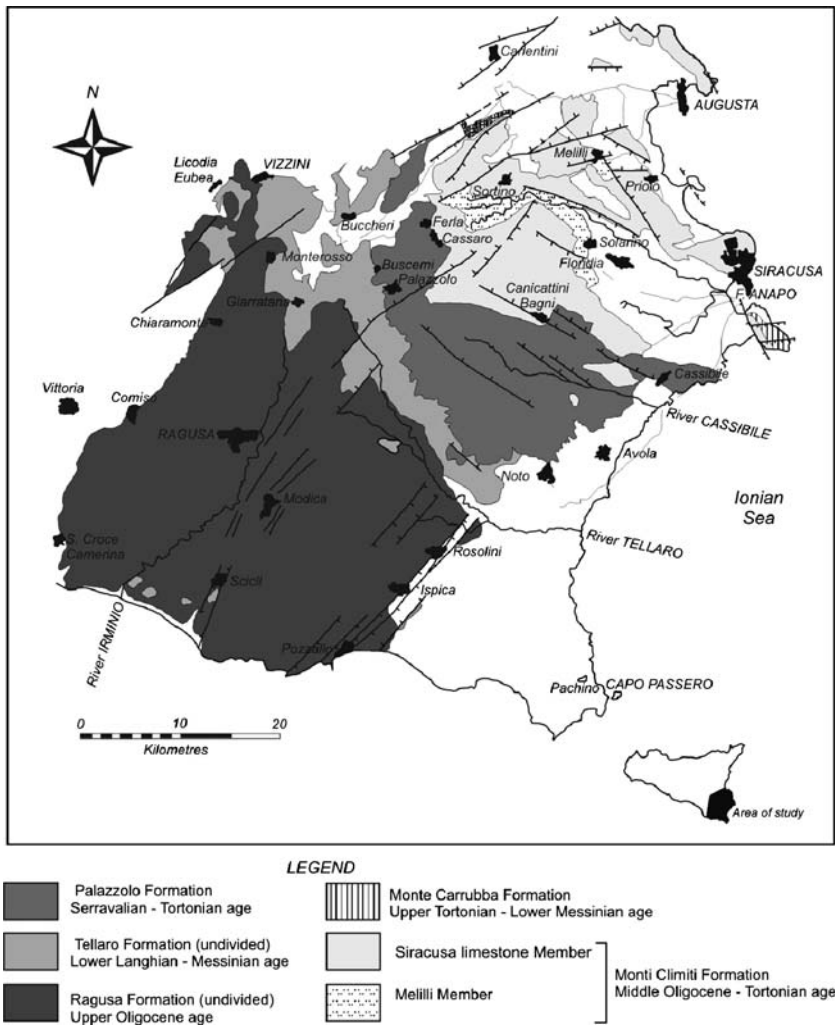

Fig. 1 Geological map of SE Sicily (from Pedley 1981, modified)

Salt crystallization test provided information on the damaging effects of soluble salts that are usually contained in water. Among these salts, commonly detected in historical buildings (Price 1996), sodium sulphate which can exist as either the anhydrous phase, thenardite, or the decahydrate mirabilite, is considered one of the most dangerous because of its strong crystallization pressure in pores and fissures (La Iglesia et al. 1997). Following UNI-EN12370 (2001), 15 test cycles of salt crystallization were performed, with a solution of 14% $NaSO_4 \times 10H_2O$, on 21 limestone samples per group. Six were subjected to the entire aging test (15 cycles). As regards the other 15 samples, every three cycles, three samples per group were analyzed to evaluate progressive deterioration.

Hydric tests were repeated after the salt crystallization test, to verify if deterioration had modified the porous system and the capacity of the rock to absorb water. These samples were first washed in distilled water to remove any traces of sodium sulphate inside them.

Distributions of pore access size and pore volume were determined on a mercury intrusion porosimeter (MIP, Micromeritics Autopore 9410) with a maximum injection pressure of 414 MPa. This apparatus can measure pores with diameters between 0.003 and 360 μm. Fresh and deteriorated cut limestone chips of about 2 cm^3 were oven-dried for 24 hat 110°C and then analyzed. Two MIP measurements per sample were carried out.

Of the techniques for determining physical properties, ultrasound stands out for its non-destructive nature. Measurements (15 in each of the three perpendicular directions) were performed on a Steinkamp BP-5 ultrasound generator with 100 kHz transducers. Pulse propagation velocity (V_P) was measured in accordance with ASTM D 2845 (1983) on dry test samples. These data were used to obtain information on the degree of compactness of samples before and after the aging test. Wave velocity was determined in controlled thermohygrometric conditions (25°C, relative humidity 50%). Structural and relative anisotropies (Guydader and Denis 1986) were calculated.

Results and discussions

Forms of deterioration of Syracuse and Melilli limestones

The first phase of this research was devoted to a detailed survey of the monuments (see Introduction), together with the evaluation of their state of deterioration. Observations were always carried out in the lower part of the façades, each submitted to similar microclimatic conditions (rainfall, orientation, etc.). ML was better preserved than SL. In more detail, SL showed selective weathering (NORMAL 1/88 1988), highlighted by characteristic algal nodules (Fig. 2); ML only suffered slight differential erosion (NORMAL 1/88 1988) especially in the Melilli monuments (Fig. 3a). In the Syracuse monuments, this form of degradation was also accompanied by superficial exfoliation, with or without swelling forms (Fig. 3b) (NORMAL 1/88 1988). Syracuse and Melilli have the same environment: a Mediterranean climate with maximum average temperatures of +30°C in summer, and +9°C in winter; higher precipitation in autumn, and an average of 427 mm of rain per year (data from http://www.eurometeo.com/).

Mineralogy and textures

Both limestones may be considered identical from the mineralogical point of view, because they are almost totally composed of calcite. Analysis of insoluble limestone residues indicated that its amount is slightly higher in ML (0.41%) than in SL (0.30%, Fig. 4). Clay and lime contents are also similar, but the sand fraction is higher in ML (Fig. 4). This analysis confirms a depositional basin in deeper water for SL (Pedley 1981).

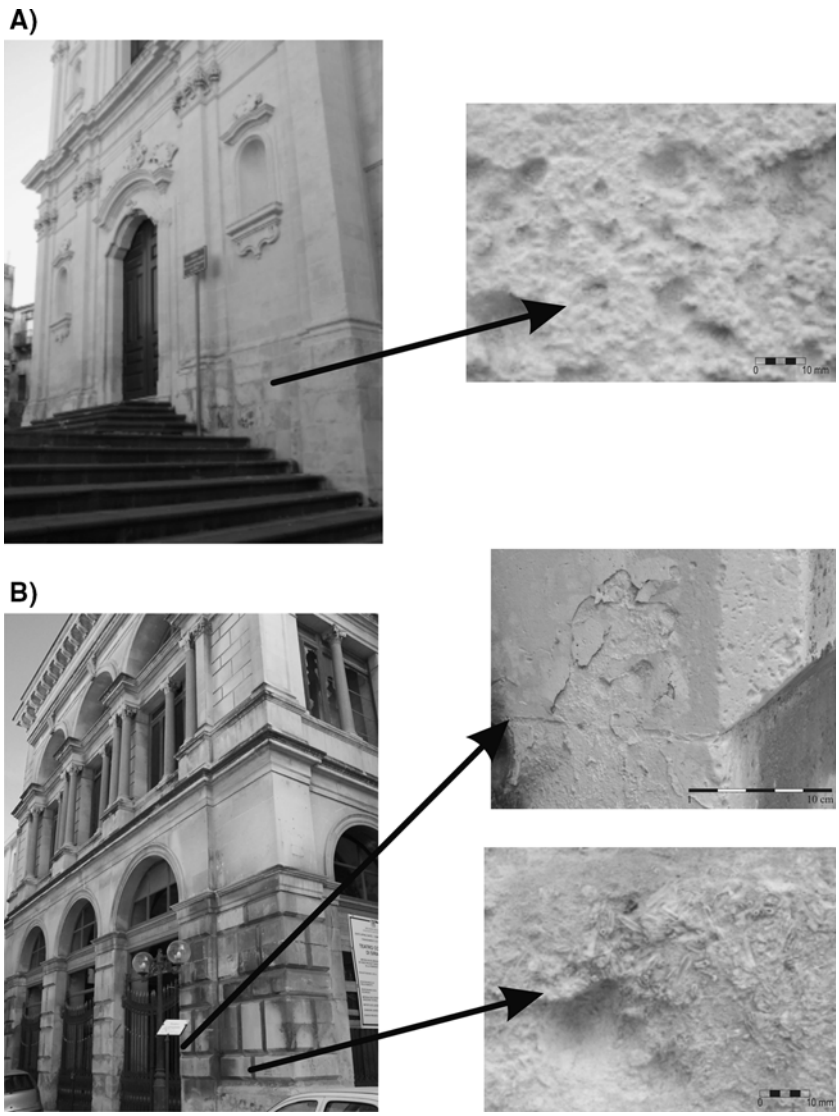

Fig. 2 Decay forms in Syracuse limestone. Athena's Temple (**a**) and Apollo's Temple (**b**) in Syracuse

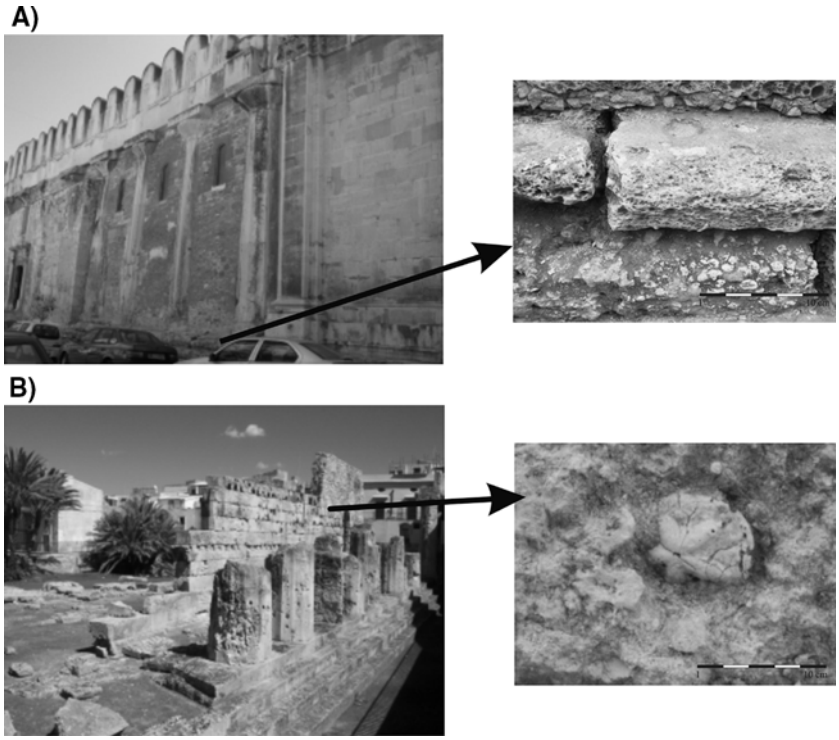

Fig. 3 Decay forms in Melilli limestone. Spirito Santo Church in Melilli (**a**) and Syracuse's Theatre (**b**)

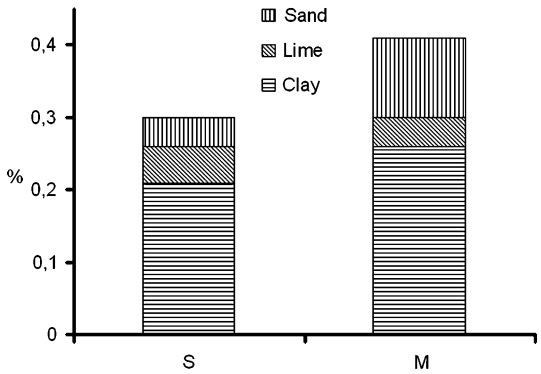

Fig. 4 Grain size distribution histogram of Syracuse (*S*) and Melilli (*M*) limestones

More differences are highlighted when the mineralogy of the clay fraction was analyzed (Fig. 5). The occurrence of smectite in both lithotypes is indicated by the expansion of the untreated d_{001} = 14.5 Å peak to 16.8 Å after glycolation, and its collapse at 10 Å on heating at 550°C. Kaolinite (d_{001} = 7.16 Å) is abundant in ML, but only traces appear in SL. Moreover, chlorite occurs only in ML, as indicated by the d_{001} = 7.16 Å kaolinite peak which disappears after heating oriented aggregates at 550°C. Small amounts of illite (d_{001} = 10 Å) also occur, but only in ML.

Quartz and francolite phases were detected in the sand and silt fractions. Quartz prevails in ML, whereas francolite is more abundant in SL.

As regard macroscopic texture, ML samples show millimetric and inhomogeneous distributed pores; SL is more compact and is characterized by smaller pores. Under the microscope, SL is a bioclastic packestone (Dunham 1962) with a fine calcirudite grain size (Fig. 6a) and grain-supported texture. Grains are composed of bioclasts and peloids. The bioclasts (40–75%) are mainly constituted of coralline algae (*Lithophyllum*) and benthic foraminifers (*Amphistegina*, *Heterostegina*), with lesser amounts of echinoid debris and *Scaphopoda* tubes. The peloids consist of carbonate grains, internally structureless, of 100–500 μm in size. They are round to subrounded, with spherical, ellipsoid or irregular morphologies. The matrix is both micro-sparitic (20–35%) and micritic (5–20%).

ML is a bioclastic wackestone (Dunham 1962), with a more homogenous texture than SL (Fig. 6b). Bioclasts represent 25% of the stone and are composed of planktonic foraminifers (*Globigerinidae*) accompanied by *Scaphopoda* tubes. Rare peloid grains are present. Intergranular spaces are filled with micro-sparite (50%) and micrite (25%).

Physical characterization

Hydric tests

The Melilli and Syracuse limestones show quite a different hydric behavior. Figure 7 shows how ML absorbs more water and reaches higher absorption values (Ca. Table 1) than SL, whereas water loss is higher in ML than in SL.

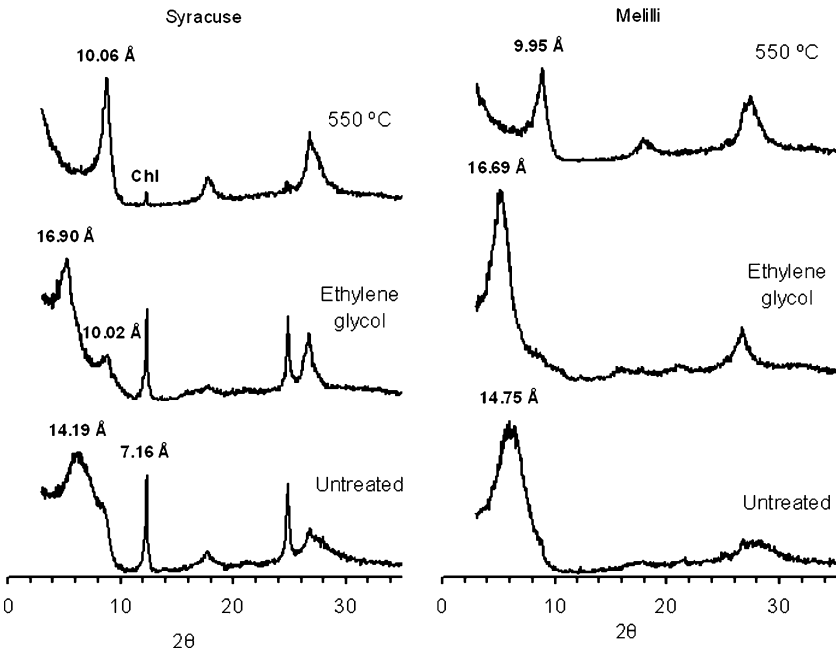

Fig. 5 X-ray diffraction patterns of clay fraction from solid residue of Syracuse and Melilli limestones (*Chl* chlorite)

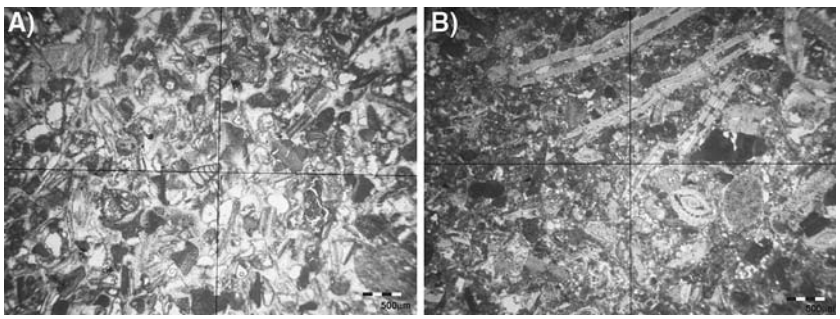

Fig. 6 Microphotographs of Syracuse (**a**) and Melilli limestones (**b**)

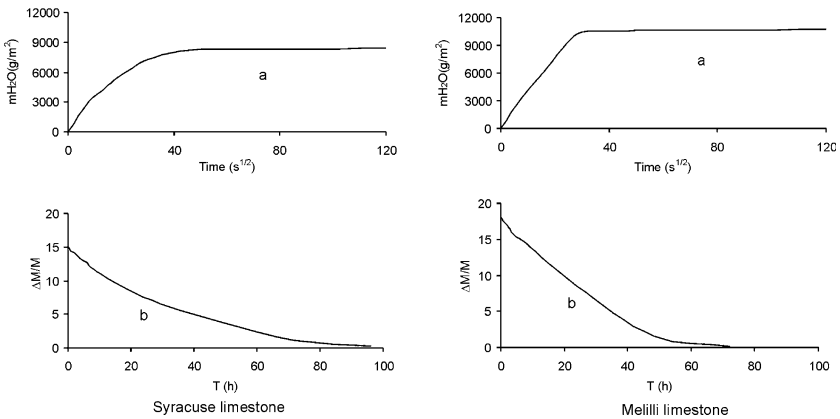

Fig. 7 Free water absorption (**a**) and desorption (**b**) curves of Syracuse (S) and Melilli limestones (M) over time

Although ML absorbs much more water (saturation coefficient C_s is higher; Table 1), it is interesting to note that it is capable of drying faster than SL (Fig. 7), indicating that there are more links among pores in ML which favor faster desorption (Cultrone et al. 2004). These results give information about vulnerability. It is precisely during drying stages, especially during the constant rate phase (Kirk and Othmer 1979), that drying stresses peak (Scherer 1990) and they mainly affect the durability of SL.

This hypothesis of the different behavior of water circulation inside the pores of SL and ML was confirmed by the calculation of the degree of pore interconnections (A_x, Table 1). As interconnectivity between pores diminishes, the difference between free and forced water absorption

Table 1 Hydric parameters and weight loss of Syracuse and Melilli limestones on fresh samples and after 6, 9 and 15 deterioration test cycles

	Syracuse limestone				Melilli limestone			
	Fresh	Deteriorated			Fresh	Deteriorated		
		Cycle 6	Cycle 9	Cycle 15		Cycle 6	Cycle 9	Cycle 15
C_a	12.84	12.66	12.68	12.13	16.55	16.44	16.05	16.16
C_c	264.18	235.15	240.13	234.49	396.37	390.69	359.41	378.45
Di	0.74	0.72	0.73	0.70	0.71	0.68	0.66	0.65
A_x	3.01	2.95	2.84	2.73	0.67	0.60	0.53	0.48
C_s	75.00	85.50	86.07	90.75	84.75	89.72	91.03	92.64
P_{HYDRIC}	21.58	23.69	25.14	25.25	27.23	27.85	28.14	29.46
ρ_r	2.51	2.45	2.46	2.45	2.52	2.46	2.47	2.49
ρ_a	1.85	1.87	1.84	1.83	1.77	1.75	1.75	1.73
M_s		2.47	6.08	8.82		0.44	0.54	0.93

C_a absorption coefficient (%), C_c capillarity coefficient (g/m^2 s$^{1/2}$), D_i drying index; A_x degree of pore interconnectivity (%), C_s saturation coefficient (%), P_{HYDRIC} open porosity (%), ρ_r real density (g/cm^3); ρ_a apparent density (g/cm^3), M_s weight loss after salt crystallization test (%)

increases, and the A_x value rises (Cultrone et al. 2004). In ML, A_x is less than 1% indicating that its pores are well connected. In SL, A_x reaches 3%, showing that here water moves with more difficulty before reaching the surface (i.e., evaporating).

Values of real density (ρ_r, Table 1) are similar in both samples, due to their almost identical mineralogy, but apparent density (ρ_a, Table 1) is lower in ML because of its higher hydric porosity (P_{HYDRIC}, Table 1). It must be recalled that this parameter was obtained by considering the value of maximum free water absorption. When the samples were submitted to forced water absorption (under vacuum), porosity values were approximately the same (27.02% for SL, 27.98% for ML).

The figure for mass absorbed by capillarity is higher in ML, which suggests that its pores are smaller, favoring capillarity rise compared with SL samples, and/or that water is prevented from rising in the latter, due to lower pore interconnections.

Salt crystallization test

At the end of this test, the average weight loss (ΔM) was 8.82% in SL and 0.93% in ML (Table 1). ML showed no evident forms of degradation, except for incipient erosion of the edges and, in only one case, initial superficial exfoliation. Instead, SL suffered general erosion (i.e., scaling). This form of decay developed after only six test cycles and behavior worsened as the number of cycles increased (Figs. 8, 9). These differences indicate that the effect of deterioration depends not only on the salt involved (the same for both materials) but also on pore size and arrangement (Colston et al. 2001).

There were some changes in hydric behavior after the aging test. No clear trend emerged as regards absorption coefficient C_a (Table 1). However, if we look at the other parameters, we see a general decrease in C_c and A_x values, confirming that deterioration modified pore structure.

Ultrasound

Fresh SL revealed faster ultrasonic wave propagation, suggesting greater compactness and higher mechanical resistance with respect to ML. Both stones were very homogeneous, as the low ΔM and Δm values indicate (Table 2). Moreover, both limestones suffered almost the same V_P loss at the end of the salt crystallization test (~15%), but behavior during testing was different

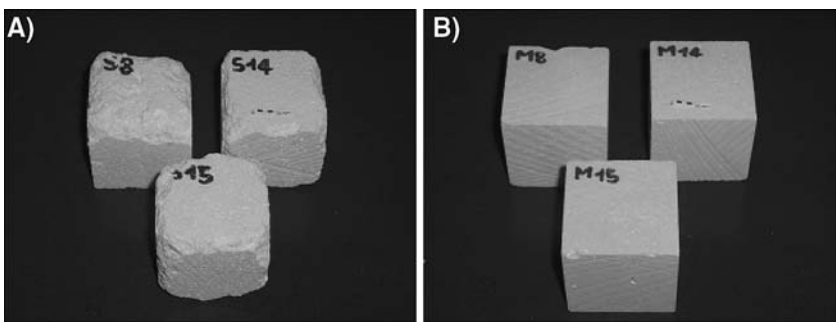

Fig. 8 Aspects of some samples of Syracuse (**a**) and Melilli (**b**) limestones after accelerated decay test

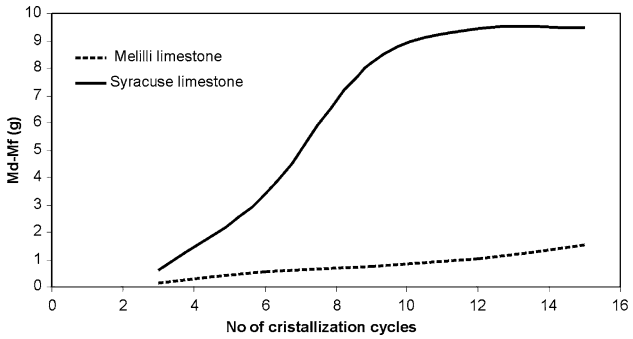

Fig. 9 Weight loss of Syracuse and Melilli samples submitted to 15 salt crystallization cycles

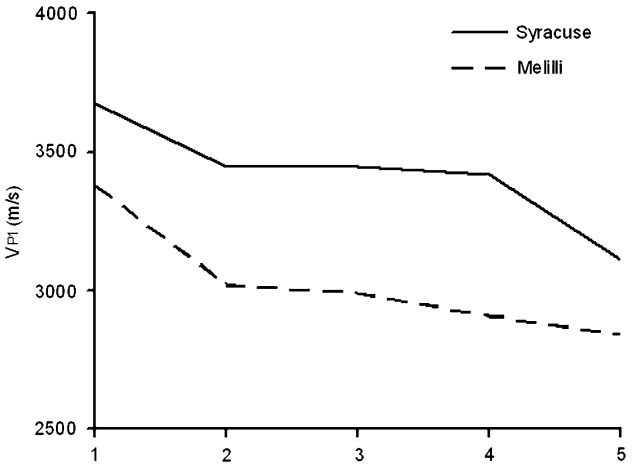

Fig. 10 Ultrasonic wave velocities of Syracuse and Melilli samples. The diagram shows the V_{P1} velocity (in m/s) versus the measurements performed at different intervals: *1* fresh samples, *2* after 3 cycles of salt crystallization test, *3* after 6 cycles, *4* after 10 cycles, *5* after 15 cycles

(Fig. 10). A first drop in V_P was evident after three test cycles (points 1 and 2) in both limestone types. Then ML revealed a slight but continuous decrease in velocity, while SL showed constant behavior between cycles 3 and 10, followed by a new drop after cycle 10. ML also maintained its isotropy during the entire test, while anisotropy increased in SL (ΔM, Table 3), suggesting the development of discontinuity surfaces (i.e., fissures). These results indicate that ML only suffers the loss of small fragments during salt crystallization, but still shows a healthy aspect. Instead, SL resists better in time but cracks, and much of its debris consists of scales, which develop selective weathering very similar to that seen in monuments.

MIP

Taking into account the pore range distribution of fresh limestone determined by MIP (Table 3), ML had a smaller number of pores with a radius of ≤0.5 μm with respect to SL (28% in the case of SL, 24% for ML). These pores are responsible for stone decay. Steiger (2005) states that crystallization pressure is effective principally in pores with entrances of 0.05 μm or smaller, and Table 4 shows how SL reaches micropore values twice as high as those of ML.

The MIP technique demonstrates why ML absorbs much more water by capillarity than SL. In fact, 0.1–2.5 μm is the pore range responsible for water absorption by capillarity (Ordóñez et al. 1997) and this range reaches 56% in ML but only 31% in SL. Moreover, comparing SL porosity data obtained by hydric and MIP tests (P_{HYDRIC} and P_{MIP}, respectively), these values are similar only if P_{HYDRIC} is calculated under vacuum, due to the low pore interconnectivity of SL. This allows us to state that both limestones have almost the same porosity.

The MIP test confirms that modifications in texture after salt crystallization cycles mainly affect SL. In fact, whereas ML has almost the same porosity and pore ranges, SL

Table 2 Speed of ultrasonic wave propagation in m/s of Syracuse and Melilli limestones

	Fresh	Deteriorated			
		Cycle 3	Cycle 6	Cycle 9	Cycle 15
Syracuse					
V_{P1}	3,676	3,449	3,446	3,421	3,112
V_{P2}	3,654	3,466	3,399	3,323	3,211
V_{P3}	3,743	3,597	3,366	3,286	3,146
ΔM	0.61	2.34	1.88	3.52	2.09
Δm	2.41	3.71	0.98	1.11	2.04
Melilli					
V_{P1}	3,378	3,022	2,992	2,910	2,838
V_{P2}	3,410	3,116	2,979	3,018	2,865
V_{P3}	3,327	3,013	3,044	2,901	2,897
ΔM	0.27	1.39	0.66	1.67	1.49
Δm	2.46	3.35	2.16	3.95	1.11

V_{P1}, V_{P2} and V_{P3} ultrasound velocities measured in three orthogonal directions, ΔM and Δm structural and relative anisotropy. Measurements were carried out on fresh samples and after 3, 6, 9 and 15 deterioration test cycles

Table 3 Pore size interval (% radii in μm) of fresh Syracuse and Melilli limestones

	>10	10–5	5–1	1–0.5	0.5–0.1	0.1–0.05	<0.05
Syracuse	19	28	21	4	18	4	6
Melilli	3	2	61	11	17	3	3

Table 4 Porometric data of Syracuse (SL) and Melilli (ML) limestones before (fresh) and after (altered) salt crystallization test

	P_{MIP}	ρ_r	ρ_a	S_a
SL fresh	28.82	2.67	1.84	3.20
SL deteriorated	35.98	2.66	1.70	4.25
ML fresh	27.87	2.42	1.78	2.85
ML deteriorated	28.23	2.43	1.74	2.97

PMIP porosity (%), ρ_r real density (g/cm^3), ρ_a apparent density (g/cm^3), S_a surface area (m^2/g)

notably modifies its pore size distribution after the 15 cycles of the accelerated aging test. In detail, in ML there is only a slight reduction of the main pore peak with $r = 2.55$ μm, and a small increase around 1 μm (Fig. 11). These changes determine an increase in total porosity of less than 2% (Table 4). Instead, SL increases its porosity by nearly 25%, has a bimodal distribution of pore radius, and the main peak of its larger pores shifts from 5 to 12 μm (Fig. 11), confirming the development of new pores/fissures as shown by the ultrasound study.

Density (ρ) and surface area (S_a) values were generally higher in SL (Table 4). ρ_r maintains the same value before and after the salt crystallization test, but ρ_a falls, mainly in SL, because of the development of new pores and/or fissures, which increase the number of empty spaces. S_a values are higher in SL because of its larger number of micropores compared with ML.

Conclusions

To a large extent, parameters such as low strength, high water absorption and microporosity affect stone durability (Benavente et al. 2004; Maage 1984; Robertson 1982), especially when the cause of damage is due to salt crystallization (Ginell 1994). However, compared with other rocks, sedimentary carbonates are known to have complex pore geometry, which commonly results in fast, intense alterations of carbonate sediments, which greatly affect pore characteristics (Anselmetti et al. 1998).

Thus, it is interesting to note that SL, the more compact and apparently less porous stone (P_{HYDRIC}, Table 1), deteriorates more easily than ML. This was found in Sicilian monuments and in our laboratory after salt crystallization tests. In addition, the disruptive effects of salt crystallization may have been partially amplified by the presence of clay minerals. McGreevy and Smith (1984) demonstrated that swelling and non-swelling clay minerals enhance salt-related breakdown and that the phenomenon is augmented by the abundance of clay in rocks. We observed that the clay concentration in Syracuse and Melilli samples was too low (<0.3%) and that the amount was slightly higher in ML, the more durable limestone. Therefore, these results do not explain the deterioration of SL.

The lesser decay of ML is explained when the speed of water loss inside the stone and the range distribution of the smallest pores are considered. These parameters determine if salt crystallization causes damaging subefflorescence or less harmful efflorescence (Rodríguez Navarro and Doehne 1999). Water is one of the most important agents of deterioration and also facilitates the damaging action of other agents (Esbert et al. 1991). McGreevy (1996) demonstrated that rapid drying of limestone allows salt solutions to migrate to and crystallize at the stone surface, causing little or no damage and that, conversely, slow evaporation promotes salt crystallization inside the stone, with a greater disruptive effect. This behavior is clear when the concepts of ease (or difficulty) of water migrating inside the stone (i.e., pore interconnections) are combined with oversaturation and the nucleation rate of salt solutions, which increase exponentially as pore size descends to zero (Kaschievic and Van Rosmalen 1995). Applying the Laplace and Washburn equation, it is demonstrated that pressure P is inversely related to pore radius r

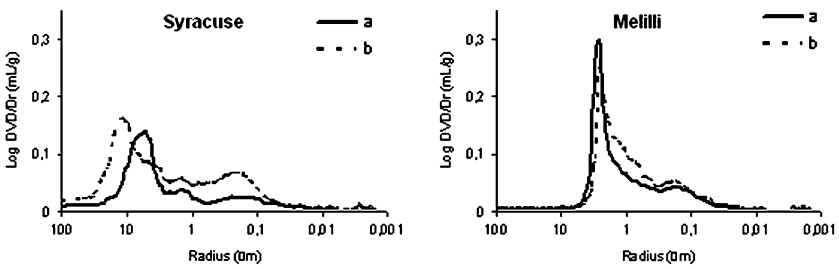

Fig. 11 MIP pore size distribution curves [i.e. log differential intruded volume (mg/l) versus pore radius (μm)] of Syracuse and Melilli limestones before (**a**) and after (**b**) salt crystallization test

$$P = 2\sigma \cos\theta / r$$

where σ is interfacial tension and θ is the contact angle of the meniscus at the pore wall. As evaporation progresses, the saturated solution which is prevented from rising to the surface is sucked from larger to smaller pores, where it concentrates, generating high crystallization pressure (Steiger 2005). Hydric and MIP tests revealed that SL has lower pore interconnections (A_x, Table 1) and large numbers of the smallest pores ($r < 50$ nm, Table 3), so that solution transport is low. This increases the possibility that high oversaturation ratios are reached below the stone surface, precipitating as subefflorescence. Instead, in ML the salt solutions can reach the surface more readily (C_c, Table 1), without reaching high oversaturation and resulting in the growth of efflorescences.

This study reveals that the characterization of construction materials is sometimes insufficient to determine the causes of deterioration if all the parameters involved are not considered. In this specific investigation, ultrasound revealed that the compactness of two construction materials, very similar from the mineralogical point of view, changed when they underwent salt crystallization attack. Hydric tests showed that the pores of Syracuse limestone were less well interconnected than those of Melilli limestone. The combination of these data with those of MIP tests explained why Syracuse limestone is more susceptible to decay.

Acknowledgments This research was supported by Research Group RNM179 of the *Junta de Andalucía*. We thank Ms Gabriel Walton for revising the English manuscript.

References

Anselmetti FS, Luthi S, Eberli GP (1998) Quantitative characterization of carbonate pore systems by digital image analysis. AAPG Bull 82:1815–1836

ASTM D 2845 (1983) Standard test method for laboratory determination of pulse velocities and ultrasonic elastic constants of rock. American Society for Testing and Materials, West Conshohocken

Benavente D, García del Cura MA, Fort R, Ordóñez S (2004) Durability estimation of porous building stones from pore structure and strength. Eng Geol 74:113–127

Bruton G (1955) Vapour glycolation. Am Mineral 40:124–126

Carbone S, Lentini F (1981) Caratteri deposizionali delle vulcanite del Miocene superiore degli Iblei (Sicilia Sud orientale). Geol Rom 20:79–101

Catalano R, Franchino A, Merlini S, Sulli A (2000) A crustal section from the Eastern Algerina basin to the Ionian ocean (Central Mediterranean). Mem Soc Geol It 55:71–86

Charola AE, Lazzarini L (1986) Material degradation caused by acid rain. In: Baboian R (ed) ACS Symposium Series n. 318. American Chemical Society, Washington, pp 250–258

Colston BJ, Watt DS, Munro HL (2001) Environmentally-induced stone decay: the cumulative effects of crystallization-hydration cycles on a Lincolnshire oopelsparite limestone. J Cult Herit 2:297–307

Cultrone G, Sebastián E, Elert K, de la Torre MJ, Cazalla O, Rodríguez Navarro C (2004) Influence of mineralogy and firing temperature on the porosity of bricks. J Eur Ceram Soc 24:547–564

Dunham RJ (1962) Classification of carbonate rocks according to depositional texture. In: Ham WE (ed) Classification of carbonate rocks. American Association of Petroleum Geologists Memoir, USA, pp 108–121

Esbert RM, Montoto M, Ordaz J (1991) Rock as construction material: durability, deterioration and conservation. Mater Construcc 41:61–73

Ginell WW (1994) The nature of changes caused by physical forces. In: Krumbein WE, Brimblecombe P, Cosgrove DE, Staniforth S (eds) Durability and change: the science, responsibility and cost of sustaining cultural heritage. Wiley, New York, pp 81–94

Grasso M (1997) Geological map of the south-central sector of Hyblean plateau (Province of Ragusa, SE Sicily) scale 1:50.000

Grasso M, Lentini F (1982) Sedimentology and tectonic evolution of the eastern Hyblean Plateau (south-eastern Sicily) during Cretaceous to Quaternary times. Palaeogeogr Palaecol 39:261–281

Grasso M, Lentini F, Lombardo G, Scamarda G (1979) Distribuzione delle facies cretaceo-mioceniche lungo l'allineamento Augusta M Lauro (Sicilia Sud-Orientale). Boll Soc Geol It 98:175–188

Grasso M, Lentini F, Pedley HM (1982) Late Tortonian–lower Messinian (Miocene) palaeogeography of SE Sicily: information from two new formations of the Sortino group. Sediment Geol 32:279–300

Guydader J, Denis A (1986) Propagation des ondes dans les roches anisotropes sous contrainte: évaluation de la qualité des schistes ardoisiers. Bull Eng Geol 33:49–55

Kashchievic D, Van Rosmalen GM (1995) Effect of pressure in bulk solutions and solutions in pores and droplets. J Colloid Surface Sci 169:214–219

Kirk RE, Othmer DF (1979) The encyclopedia of chemical technology. Diuretics to Emulsions, vol 8, 3rd edn. Wiley, New York

Kowalski WC (1975) L'influence des variations de teneur en eau sur la resistance mécanique et la déformation des roches dans la zone d'altération. Bull Assoc Intern Geol Ingen 12:37–43

La Iglesia A, González V, López Acevedo V, Viedma C (1997) Salt crystallization in porous construction materials I Estimation of crystallization pressure. J Cryst Growth 177:111–118

Maage M (1984) Frost resistance and pore size distribution in bricks. Mater Struct 17:345–350

McGreevy JP (1996) Pore properties of limestones as controls on salt weathering susceptibility: a case study. In: Smith BJ, Warke PA (eds) Processes of Urban Stone Decay, vol 4. Dohnead, New York, pp 150–167

McGreevy JP, Smith BJ (1984) The possible role of clay minerals in salt weathering. Catena 11:169–175

Moore DM, Reynolds RC (1989) X-Ray diffraction and the identification and analysis of clay minerals. Oxford University Press, UK

NORMAL 7/81 (1981) Assorbimento d'acqua per immersione totale. Capacità di imbibizione. CNR-ICR, Rome, Italy

NORMAL 1/88 (1988) Alterazioni macroscopiche dei materiali lapidei: lessico. CNR-ICR, Rome, Italy

NORMAL 29/88 (1988) Misura dell'indice di asciugamento (drying index). CNR-ICR, Rome, Italy

Ordóñez S, Fort R, Garía del Cura MA (1997) Pore size distribution and the durability of a porous limestone. Q J Eng Geol 30:221–230

Pedley HM (1981) Sedimentology and paleoenvironment of the south-east Sicilian Tertiary platform carbonates. Sediment Geol 28:273–291

Price CA (1996) Stone conservation An overview of current research. The Getty Conservation Institute, Santa Monica

Robertson WD (1982) Evaluation of the durability of limestone masonry in historic buildings Preprints of the contributions to the Washington Congress "Science and technology in the service of conservation". International Institute for Conservation of Historic and Artistic Works, Washington, pp 51–55

Ragg S, Grasso M, Müller B (1999) Patterns of tectonic stress in Sicily derived from borehole breakout analysis. Tectonics 18:669–685

Rigo M, Barbieri F (1959) Stratigrafia pratica applicata in Sicilia. Boll Serv Geol It 80:351–442

Rodríguez Navarro C, Doehne E (1999) Salt weathering: influence of evaporation rate, supersaturation and crystallization pattern. Earth Surf Proc Land 24:191–209

Scherer GW (1990) Theory of drying. J Am Ceram Soc 73:3–14

Steiger M (2005) Crystal growth in porous materials II: Influence of crystal size on the crystallization pressure. J Cryst Growth 282:470–481

UNI-EN 1925 (2000) Metodi di prova per pietre naturali. Determinazione del coefficiente di assorbimento d'acqua per capillarità. CNR-ICR, Rome, Italy

UNI-EN 12370 (2001) Metodi di prova per pietre naturali. Determinazione della resistenza alla cristallizzazione dei sali. CNR-ICR, Rome, Italy

Yellin-Dror A, Grasso M, Ben Avraham Z, Tibor G (1997) The subsidence history of the northern Hyblean plateau margin, southeastern Sicily. Tectonophysics 282:277–289